REPORT DOCUMENTATION PAGE

AFRL-SR-AR-TR-08-0287

1. REPORT DATE *(DD-MM-YYYY)* 08-05-2008	**2. REPORT TYPE** Final Technical	**3. DATES COVERED** *(From - To)* 01 Mar 2004 - 31 May 2007
4. TITLE AND SUBTITLE High Performance and High-Fidelity Aeroelastic Simulation of Fixed Wing Airicraft with Deployable Control Surfaces		**5a. CONTRACT NUMBER**
		5b. GRANT NUMBER FA9550-04-1-0084
		5c. PROGRAM ELEMENT NUMBER
6. AUTHOR(S) **Dr. Michel Lesoinne**		**5d. PROJECT NUMBER**
		5e. TASK NUMBER
		5f. WORK UNIT NUMBER
7. PERFORMING ORGANIZATION NAME(S) AND ADDRESS(ES) University of Colorado Boulder, CO 80309		**8. PERFORMING ORGANIZATION REPORT NUMBER**
9. SPONSORING / MONITORING AGENCY NAME(S) AND ADDRESS(ES) USAF/AFRL AFOSR/NA 875 N Randolph St Ste 3112 Arlington VA 22031 Dr John Schmisseur		**10. SPONSOR/MONITOR'S ACRONYM(S)**
		11. SPONSOR/MONITOR'S REPORT NUMBER(S)

12. DISTRIBUTION / AVAILABILITY STATEMENT

Distribution A; Approved for public release; distribution is unlimited

13. SUPPLEMENTARY NOTES

14. ABSTRACT

The goals of this research is to overcome the difficulties created by mesh shearing in the simulation of aircraft with large control surface deflection. The origin of the difficulties for the correct modeling of large control surface deflection is that they introduce shearing in the mesh at the place where the control surface meets the fixed part of the wing. Such a geometrical shearing is very difficult to handle, in particular in Finite Volume or Finite Element approaches. One option to tackle this problem is the use of Chimera grids. However Chimera grid approaches are relatively expensive in geometric computation and introduce an interpolation error due to the overlap of the grids. We have proposed to explore two alternate methods to tackle this issue: Meshfree methods and Level-Set Methods. At the end of the project, we had demonstrated that the node activation/de-activation method worked on a sample one dimensional problem and the implementation in two dimensions is still in progress.

15. SUBJECT TERMS

16. SECURITY CLASSIFICATION OF:			**17. LIMITATION OF ABSTRACT**	**18. NUMBER OF PAGES**	**19a. NAME OF RESPONSIBLE PERSON** Michel Lesoinne
a. REPORT U	**b. ABSTRACT** U	**c. THIS PAGE** U	UU	13	**19b. TELEPHONE NUMBER** *(include area code)*

Final report on project titled "High Performance and High-Fidelity Aeroelastic Simulation of Fixed Wing Aircraft with Deployable Control Surfaces"

Michel Lesoinne
Department of Aerospace Engineering Sciences
and Center for Aerospace Structures
University of Colorado at Boulder

October 9, 2007

1 Introduction

The goals of this research is to overcome the difficulties created by mesh shearing in the simulation of aircraft with large control surface deflection. The origin of the difficulties for the correct modeling of large control surface deflection is that they introduce shearing in the mesh at the place where the control surface meets the fixed part of the wing (see Fig. 1). Such a geometrical shearing is very difficult to handle, in particular in Finite Volume or Finite Element approaches. One option to tackle this problem is the use of Chimera grids.However Chimera grid approaches are relatively expensive in geometric computation and introduce an interpolation error due to the overlap of the grids. We have proposed to explore two alternate methods to tackle this issue:

1. Meshfree Methods.
2. Level-Set Methods.

During the first year of this research, we developed the Meshfree method for aeroelastic problems and created a new approach to dealing with Neumann Boundary Conditions. We then proceeded to implement this approach in two dimensions and showed initial aeroelastic results for an airfoil moving in a forced pitching motion. The experiments showed that the method worked, though the cost of the method tended to indicate that its use should be limited to areas where other methods would not be appropriate.

In the second year, we then tackled the problem of Control Surface Deployment. This effort resulted in some partial success. However, new problems surfaced with conditioning of the resulting system and we started the level-set type approach to avoid the ill-conditioning problem. This approach has shown

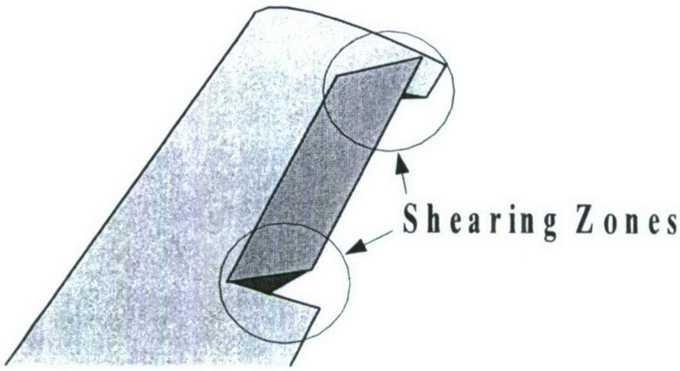

Figure 1: Mesh Shearing Regions due to Control Surface Deflections

good results for any geometry and at the end of the project, work was continuing in implementing the full time dependent solution of problems with moving control surfaces.

2 The Meshless Approach to Aeroelasticity

2.1 The reasons for a Meshless Approach to Aeroelasticity

We have chosen to approach the problem of simulating aircraft with large control surface deflection with a Meshless Approach. Meshless methods have been applied to problems from Crack propagation to Astrophysics and Fluid problems. In general, such methods are particularly adapted where the boundary of the computational domain greatly evolves during the time of the simulation.

Meshless Methods are particularly adapted to problems where the boundary significantly evolves in time, because they never require to form or maintain a mesh topology. Unlike Finite Element or Finite Volume methods, where the motion of nodes is constrained by the necessity to preserve positivity of the volumes of the discretization elements, the Meshless Methods can accept almost arbitrary relative motions of all the nodes.

The only constrain imposed on the relative motion of the nodes is that a sufficient number of nodes are close to any point in the domains, so that the interpolation functions are well defined for every point in the domain. The exact number of nodes and the definition of *close* depends on the particular variant of Meshless Methods being used. In general, such constraints are rather weak and can easily be enforced with no significant difficulty.

These facts are major advantages for the Meshless Approaches when applied to Aeroelasticity problems. This is true, not only when large control surface deflections are present, but also when large relative motions of objects have to be simulated. Examples of such problems are Missile Separation problems, Ejection Seat simulations and Formation Flying of several aircraft.

2.2 Advantages of Meshless Approaches to Aeroelasticity

- Ease of handling arbitrary relative motion of boundaries. Because meshless methods do not require to maintain a topological coherence to the mesh, nodes can be moved almost arbitrarily relative to one another.

- Ease of refining the solution by inserting new nodes. New nodes can easily inserted to refine the solution where high gradients are observed. The insertion does not require, as in FE or FV methods to construct a new mesh topology.

2.3 Disadvantages of Meshless Approaches to Aeroelasticity

The major disadvantages of Meshless Approaches when applied to Aeroelastic problems are:

- Cost: The computation of the shape functions with some methods (for example RKPM) is much more expensive than a Finite Element equivalent.

- Essential Boundary Conditions: Imposing Essential Boundary Conditions in Meshless Methods is not a trivial matter. This is shared with all Meshless methods and is due to the fact that the value of the solution at a computational node is not equal to the value of the node. Or phrased mathematically, the Meshless shape functions do not exhibit a Kronecker delta property.

- Complexity of integration, choosing Gauss Points and finding nodes with influence over the Gauss Points.

3 Results on Meshless Methods

A graduate student, Vivek Kaila, was recruited to work on this project and began working March 1st 2004. Our approach is based on the use of the Reproducing Kernel Particle Method combined with the Streamline Upwind Petrov-Galerkin (SUPG) method.

3.1 RKPM Approach

Of the various methods that exist in the literature on Meshless Methods, we chose to concentrate on the Reproducing Kernel Particle Method (RKPM), due its use by other researchers in CFD problems. The research did not seek to be on the chosen Meshless Method, but on the adaptation of Meshless Methods to Aeroelastic problems. The developments made in this research are, and should remain, applicable to any Meshless Method.

Common to all Meshless Methods, the solution is constructed from some nodal *values*[1] U_I and shape functions $\Phi_I(x)$ are constructed for each node. The solution is then given by:

$$U(x) = \sum_I \Phi_I U_I \tag{1}$$

The difference between the different existing methods is in the construction and resulting properties of the shape function. We note that the difficulty in the imposition of essential boundary conditions is a result of the fact that $\Phi_I(x_J) \neq \delta_{IJ}$ where x_J is the location of node J.

3.2 Imposing Boundary Conditions

As was mentioned before, the main difficulty with Meshless Methods is to impose Essential Boundary Conditions. Several existing approaches were considered but were deemed unsatisfactory:

- Lagrange Multiplier Methods: Such methods impose the essential boundary conditions in a weak manner. Either by collocation – in which case the boundary conditions are satisfied only at a discrete set of points – or in an average form. The resulting solution is equivalent to having solved the problem around a slightly different structure than the intended one.

- Blending of Meshless and Finite Element methods: Such methods which transition the Meshless solution to a Finite Element (FE) solution on the boundary do not suffer of the aforementioned problem. However, if refinement of the solution is needed, they require a re-meshing of the FE mesh near the boundary to capture the same fine solution as in the Meshless Domain. Such re-meshing is much more expensive to perform than the insertion of nodes in the Meshless approach and requires an added interpolation of the solution between meshes, if this operation is performed during a time dependent simulation.

We decided to design a new method for the imposition of the Essential Boundary Conditions, with the following features:

- The method should preserve the spatial resolution of the Meshless solution without severe difficulties.

- It must impose the boundary condition strongly on the entire boundary.

- It must be easy to adapt for boundary surfaces undergoing arbitrary and potentially large relative motions.

Our efforts have resulted in the design of a Projection Based Boundary Condition treatment which we will now describe below:

[1] These values are *associated with the node* but are not the value of the solution *at* the node.

Though we have started with the inviscid flow condition, and will only present this case in what follows, the method extends fairly easily to viscous flows.

In inviscid flows, the common type of boundary condition is the *slip* condition, where the flow must be tangent to the airfoil or wing surface. Such a condition, in the presence of a structural velocity at the interface $\vec{u}_s$ stipulates that the flow velocity $\vec{u}_f$ must be such that:

$$\vec{u}_f \cdot \vec{n} = \vec{u}_s \cdot \vec{n} \quad \text{on } \Gamma_{F/S} \tag{2}$$

Let us remind the reader that the solution quantities are given by the conservative variable vector which in two dimensions is given by:

$$U = \begin{pmatrix} \rho \\ \rho u \\ \rho v \\ \rho E \end{pmatrix} \tag{3}$$

where u v are the components of the velocity vector and E is the total energy density.

We then notice that given a solution U_M that would be obtained by the Meshless Approach, we can build a solution U that satisfies the Boundary Condition by the use of a project:

$$U = PU_M + Qu_s \tag{4}$$

where

$$P = \begin{pmatrix} 1 & 0 & 0 & 0 \\ 0 & 1 - n_x n_x & -n_x n_y & 0 \\ 0 & -n_x n_y & 1 - n_y n_y & 0 \\ 0 & 0 & 0 & 1 \end{pmatrix}$$

and

$$Q = \begin{pmatrix} 0 & 0 \\ n_x n_x & n_x n_y \\ n_x n_y & n_y n_y \\ 0 & 0 \end{pmatrix}$$

It is therefore possible to construct a continuous solution by gradually *blending* the modified solution given by equation 4 and the meshless solution U_M.

In the presence of a single surface, we define a ramping function $r(x)$ which is such that $r(x) = 1$ on $\Gamma_{F/S}$ and becomes 0 away from the surface. Then the solution is given by:

$$U = ((1 - r(x))I + r(x)P)U_M + r(x)u_S \tag{5}$$

The ramping function must transition between 0 and 1 around the interface in a distance compatible with the expected resolution of the Meshless Method.

The method can then be extended to multiple surfaces by creating one ramping function that satisfy that the ramping function $r_i(x)$ for surface i is 0 away from that surface and also on any other boundary surface, while it is 1 on its respective surface.

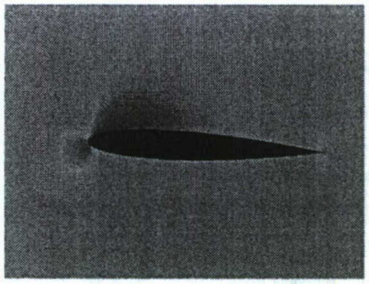

Figure 2: Pressure contours at M=0.6 on a 2000 node Mesh

4 Difficulties with the Meshless Method

Though, overall, the Meshless Method seems to perform reasonably well. However, when control surfaces are deployed, as the nodes attached to the various components follow them in their motion, nodes attached to one component can get extremely close to nodes associated with another component. As a result, two problems became evident as more simulations were performed and time dependent with control surface deployment problems were explored:

- on coarse mesh, the solution exhibits unacceptable oscillations.
- as the flap angle changes, node getting close create a very ill-conditioned system.

The second problem is a major one and can easily be understood because the equation for the shape functions starts exhibiting extremely strong local gradients when nodes get too close to one another. The first problem is linked to the second and is exhibited in figure 4 Consequently, it was realized that some method would have to be developed so that solution from different meshes are not active in the same area to avoid this problem. It seemed that a level-set type method used to blend the solution from two meshes would provide a reasonably inexpensive solution to this problem.

5 Levelset Method

The levelset method is used to blend the solution of two meshes as shown in figure 5 For each mesh, we created two levelset methods, Φ_i and Ψ_i:

- Φ is akin to the *Distance* from the airfoil
- $\Phi_i = 0$ on Γ_i; $\Phi_i = 1$ on far-field i
- Ψ is akin to the *Distance* from Non-Physical Mesh boundary

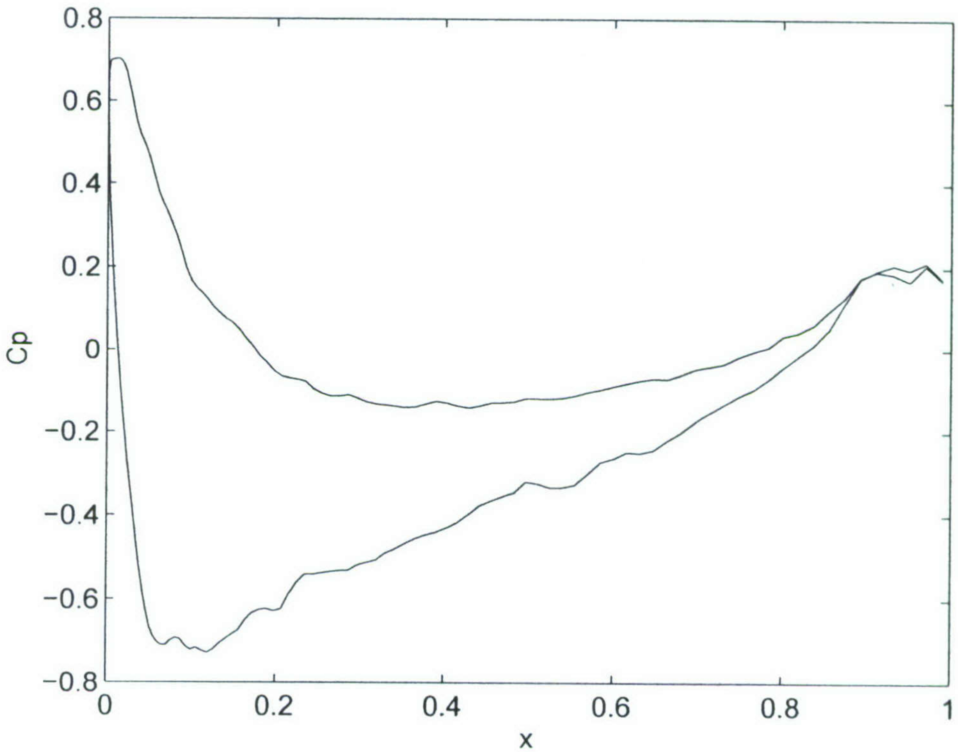

Figure 3: C_p contour on an airfoil with a deflected control surface

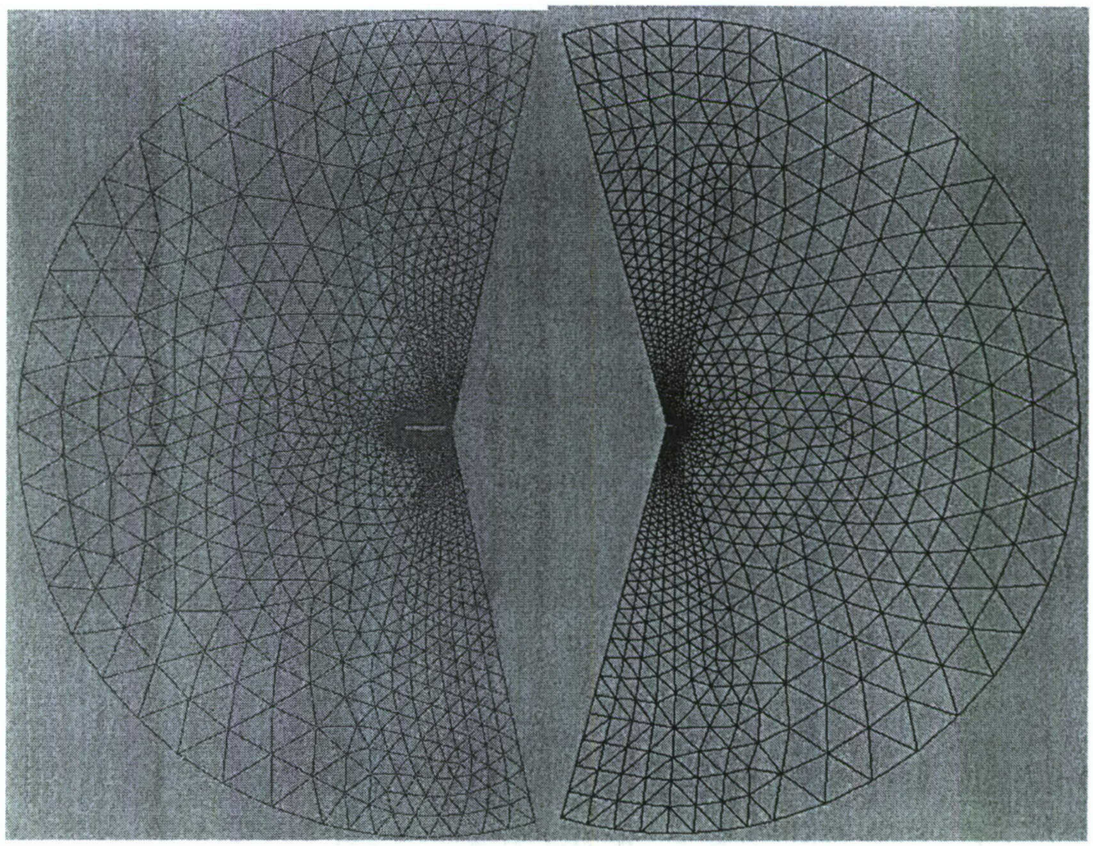

Figure 4: The airfoil and flap meshes

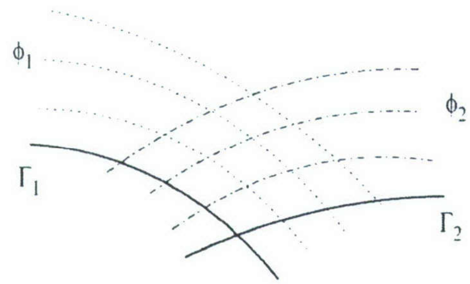

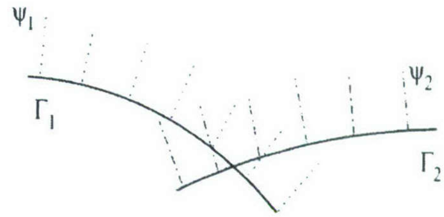

Figure 5: Level set functions

Both functions are created by solving a simple Laplace problem. Figure fig:phipsi shows the contours of such functions. The level-set functions are then used to blend the solutions U_1 and U_2 from both meshes: Let:

$$D_1 = \frac{\Psi_1 - \Psi_2 - d}{c} + \frac{1}{2} \tag{6}$$

and

$$D_2 = 1 - D_1 \tag{7}$$

In these equations, d is a function of the angular deflection of the flap and measures the difference $\Psi_1 - \Psi_2$ at the intersection points of the meshes. c is a parameter to adjust the width of the transition and the function D_1 and consequently D_2 are then clamped between 0 and 1/

We then define thee influence coefficients for each mesh, s_1 and s_2:

$$S_1 = \frac{\Phi_2(1-\Phi_1)/D_2}{\Phi_2(1-\Phi_1)/D_2 + \Phi_1(1-\Phi_2)/D_1} \quad ; \quad S_2 = 1 - S_1$$

Finally, we use these functions to blend the the two mesh solutions:

$$U = S_1 U_1 + S_2 U_2$$

Figure 5 and 5 shows the contours of $S_1 = 0.9$, $S_1 = 0.5$ and $S_1 = 0.1$ from left to right.

5.1 Node activation and de-activation

One notes that for some nodes, the S_i function associated with their mesh, will be identically zero over the whole domain of influence of the node. Such nodes will thus have no contribution to the solution and are to be de-activated from the solution process.

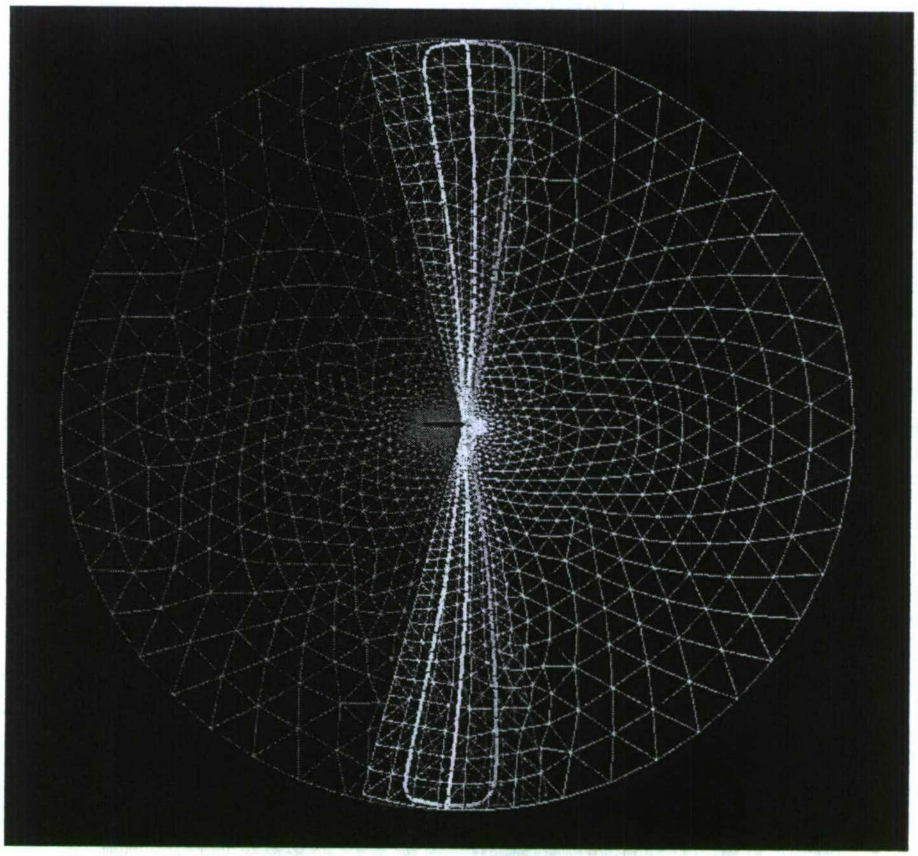

Figure 6: Contours of the S_1 function

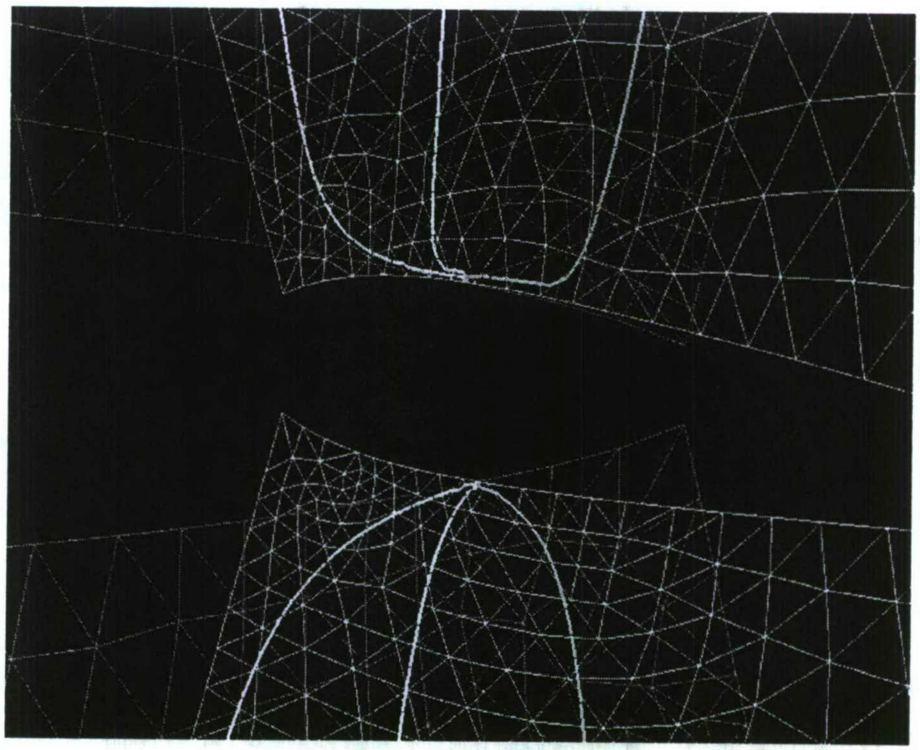

Figure 7: Close-up of the contours of the S_1 function

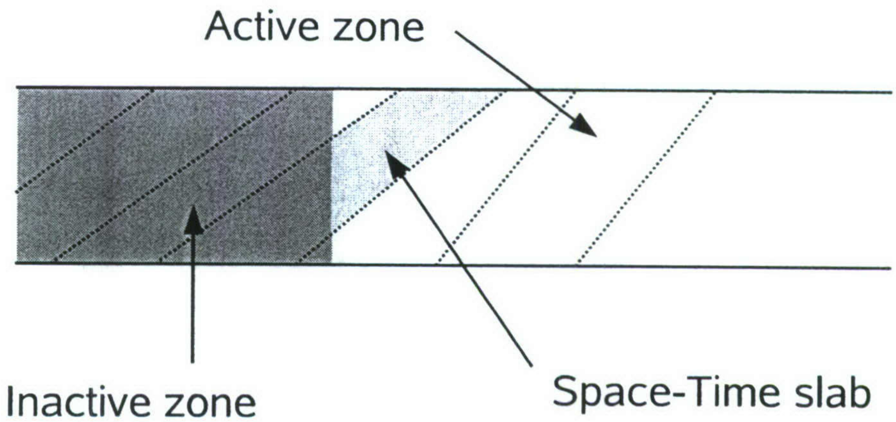

Figure 8: One dimensional Space-Time slabs associated with a single mesh

We also note that, as the angle of deflection of the control surface varies in time, nodes can become inactive or active over time. It is therefore necessary to devise a procedure to deal with this issue. The approach we devised to treat the node activation and de-activation is based on the notion of space-time slabs. One first notes that the time integration can generally be written in the form of a time integral that combines with the space integration. For node I, we will have an integral of the form:

$$\int_{t^n}^{t^{n+1}} \int_{\Omega} \Phi_I(x,t)(\frac{\partial U}{\partial t} + \cdots) d\Omega dt \tag{8}$$

And $\Phi_I(x,t)$ is a test function associated with node I. In general, this test function will be zero where node I has no influence in space time. Figure 5.1 shows for a one dimensional problem the active part of the space-time slab for an element. This figure also illustrates the fact that a node may be inactive at time-step n while it becomes active at time-step $n+1$. In such a case, before we proceed with the integration from t^n to t^{n+1}, the variables associated with an inactive node have no value. Consequently, in the time integration between time t^n and t^{n+1}, for a previously inactive node, both U_I^n and U_I^{n+1} are unknown. For such nodes, we have to write two versions of equation 8 with the shape functions Φ_I^n and Φ_I^{n+1}.

The additional equations, associated with the test function Φ_I^n provide the required number of equation to completely solve the problem.

6 Status

At the end of the project, we had demonstrated that the node activation/deactivation method worked on a sample one dimensional problem and the implementation in two dimensions is still in progress.

7 Publications

- *A Meshless Method for Aeroelastic Simulations with large Control Surface Deflections*, M. Lesoinne and V. Kaila, 6th World Conress of Computational Mechanics, Beijing, China, September 2004.
- *Meshless Aeroelastic Simulations of Aircraft with Large Control Surface Deflections*, M. Lesoinne and V. Kaila, 43rd AIAA Aerospace Sciences Meeting and Exhibit, Reno, NV, January 2005.